ECCOMAS Congress 2016
VII European Congress on Computational Methods in Applied Sciences and Engineering
M. Papadrakakis, V. Papadopoulos, G. Stefanou, V. Plevris (eds.)
Crete Island, Greece, 5–10 June 2016

DEFORMATION-DIFFUSION COUPLED ANALYSIS OF LONG-TERM HYDROGEN DIFFUSION IN NANOFILMS

X. Sun[1], **M. P. Ariza**[2] **and K. G. Wang**[1]

[1] Department of Aerospace and Ocean Engineering, Virginia Polytechnic Institute and State University
Blacksburg, VA 24061, USA
e-mail: {xssun, kevinwgy}@vt.edu

[2] Escuela Técnica Superior de Ingeniería, Universidad de Sevilla
Sevilla 41092, Spain
mpariza@us.es

Keywords: Deformation-Diffusion Coupling, Non-Equilibrium Statistical Mechanics, Mean-field Theory, Discrete Kinetic Law, Long-Term Processes, Hydrogen Diffusion.

Abstract. *The absorption and desorption of hydrogen in nanomaterials can be characterized by an atomic, deformation-diffusion coupled process with a time scale of the order of seconds to hours. This time scale is beyond the time windows of conventional atomistic computational models such as molecular dynamics (MD) and transition state theory based accelerated MD. In this paper, we present a novel, deformation-diffusion coupled computational model basing on non-equilibrium statistical mechanics, which allows long-term simulation of hydrogen absorption and desorption at atomic scale. Specifically, we propose a carefully designed trial Hamiltonian in order to construct our meanfield based approximation, then apply it to investigate the palladium-hydrogen (Pd-H) system. Specifically, here we combine the meanfield model with a discrete kinetic law for hydrogen diffusion in palladium nanofilms. This combination in practice defines the evolution of hydrogen atomic fractions and lattice constants, which facilitates the characterization of the deformation-diffusion process of hydrogen over both space and time. Using the embedded atom model (EAM) potential, we investigate the deformation-diffusion problem of hydrogen desorption and absorption in palladium nanofilms and compare our results with experiments both in equilibrium and non-equilibrium cases.*

1 INTRODUCTION

In a large number of areas, the behavior of material systems depends sensitively on properties that pertain to the atomistic scale. Thus, nanotechnology has made an extensive contribution to opening up novel frontiers in material science and engineering, particularly in the design and manufacture of more efficient and reliable materials for energy storage applications. Due to its high-energy, easy availability, and non-toxicity, hydrogen is a promising energy carrier as a potential substitute for fossil fuels in future transport applications. In particular, the storage of hydrogen in metals is one of the technologies that has been the focus of extensive research. However, there exist some failure phenomena in hydrogen-metal systems that constitute the main barriers against their use in the large scale. Hydrogen embrittlement is one of the most common failure processes, which reduces the mechanical properties of metals due to the inclusion of hydrogen atoms [1, 2]. In order to prevent most of the failures associated to the degradation of metals, a natural starting point is to characterize and understand the hydrogen transport process in metals. This gives rise to the development of predictive design of nanostructured materials for hydrogen-storage.

The absorption and desorption of hydrogen in nanomaterials is characterized by an atomic deformation-diffusion process on a length scale of Angstroms and a time scale of femtoseconds. Nonetheless, the properties and behaviors of interest in real-world engineering applications (e.g. fuel cell vehicles) are macroscopic and take place on the scales of centimeters to meters, and are characterized by a relatively slow evolution on the scale of seconds to years. This vast disparity of length and time scales poses extraordinary challenges in theoretical and computational material science, as well as material design. Most computational efforts up to date have relied on traditional first-principles-based Molecular Dynamics (MD) or Monte Carlo (MC) methods [3, 4] as their chief representational and computational paradigm. However, these two computational methods are limited to relatively small material samples and to time windows of microseconds at best. Considerable efforts have been devoted to accelerating MD and MC methods, such as accelerated MD [5, 6] and diffusive MD [7]. However, no computationally-tractable atomistically-based models appear to be available to study deformation-diffusion coupled problems with the vast disparity of length and time scales described above.

Our objective in this work is to enable long-term (e.g., up to seconds), predictive simulation of hydrogen absorption and desorption in metal-based nanomaterials, while maintaining a strictly atomistic description of the material. To achieve this objective, we apply the atomistic-continuum coupling approach proposed in Ref. [8]. In Ref. [8], a non-equilibrium statistical thermodynamics theory is proposed for multi-species particulate solids based on Jayne's maximum entropy principle and the meanfield approximation approach that allow the statistical treatment of systems away from equilibrium. Unlike in MD and MC, the individual hops of atoms are not explicitly tracked, but instead accounted for in the theory in a statistical sense. Most recently, this theoretical model has been applied to simulate hydrogen diffusion in Pd nanofilms [9]; however, the Pd sub-system was assumed to be rigid, and the phase-dependent deformation of the sample during hydrogen absorption/desorption was not accounted for.

This work is an extension of Ref. [9] to long-term, atomistic, deformation-diffusion coupled analysis. The metal (e.g. Pd) sub-system is no longer assumed rigid. Instead, using the non-equilibrium statistical thermodynamics model proposed in Ref. [8], the deformation of metal hydride will be characterized by the time-dependent mean atomic positions of both metal and hydrogen atoms. The empirical discrete kinetic model will be developed by extending the Fick's laws for continuum, and calibrated against experimental data and results obtained by first-principle simulations. The organization of the paper is as follows. Section 2 generalizes the non-equilibrium statistical model with the carefully designed trial Hamiltonians. In Section 3, we

will validate the proposed model of H diffusion in Pd nanofilms, accounting for both equilibrium and non-equilibrium cases. A summary of this work is finally presented in Section 4.

2 NON-EQUILIBRIUM STATISTICAL MODEL

We combine the atomistic-continuum coupling approach proposed in Ref. [8] with a novel meanfield trial model. This non-equilibrium statistical thermodynamics theory is proposed for multi-species particulate solids based on Jayne's maximum entropy principle and the meanfield approximation approach that can deal with a non-equilibrium problem.

2.1 Non-equilibrium statistical mechanics

We consider a discrete system consisting of N particle sites, each of which can be occupied by one of M species. At each particle site $i = 1, 2, \ldots, N$, and for each species $k = 1, 2, \ldots, M$, we introduce an *occupancy function* defined as

$$n_{ik} = \begin{cases} 1 & \text{if the site } i \text{ is occupied by the species } k \\ 0 & \text{otherwise} \end{cases} \tag{1}$$

Thus, the microscopic states of the system can be defined by the instantaneous positions $\{\boldsymbol{q}\} = (\boldsymbol{q}_i)_{i=1}^{N}$, momenta $\{\boldsymbol{p}\} = (\boldsymbol{p}_i)_{i=1}^{N}$, and occupancy arrays $\{\boldsymbol{n}\} = (\boldsymbol{n}_i)_{i=1}^{N}$. It is assume that the statistics of the system obeys Jaynes' principle of maximum entropy [10, 11], namely maximizing the information-theoretical entropy

$$S[\rho] = -k_{\mathrm{B}} \langle \log \rho \rangle \tag{2}$$

among all probability measures of $\rho(\{\boldsymbol{q}\}, \{\boldsymbol{p}\}, \{\boldsymbol{n}\})$. k_{B} indicates Boltzmann's constant and $\langle A \rangle$ denotes the expected value of the observation A. We specifically consider the system consisting of distinguishable particles whose Hamiltonians have the additive structure of local Hamiltonian h_i. Suppose that the expected particle energies and the expected particle atomic fractions on each atomic site are known, namely

$$\langle h_i \rangle = e_i, \ \langle n_{ik} \rangle = x_{ik} \tag{3}$$

for $i = 1, 2, \ldots, N$ and $k = 1, 2, \ldots, M$. It is worth noting that different from the classical equilibrium framework where only global constraints are enforced, here constraints are now local. Maximizing Eq. (2) with local constraints among probability measures results, after a straightforward calculation, in

$$\rho = \frac{1}{\Xi} \mathrm{e}^{-\{\beta\}^T \{h\} + \{\gamma\}^T \{\boldsymbol{n}\}} \tag{4}$$

where

$$\Xi = \sum_{\{\boldsymbol{n}\} \in O_{NM}} \frac{1}{h^{3N}} \int_{\Gamma} \mathrm{e}^{-\{\beta\}^T \{h\} + \{\gamma\}^T \{\boldsymbol{n}\}} \mathrm{d}\boldsymbol{q} \mathrm{d}\boldsymbol{p} \tag{5}$$

and $(\{\beta\}, \{\boldsymbol{\gamma}\})$ are Lagrange multipliers. h is Planck's constant. By comparison with equilibrium statistical mechanics, we may interpret Eq. (4) and Eq. (5) as non-equilibrium generalizations of the Gibbs grand-canonical probability density function and the grand-canonical partition function, respectively. Also, we may regard $T_i = 1/(k_{\mathrm{B}}\beta_i)$ and $\boldsymbol{\mu}_i = k_{\mathrm{B}} T_i \boldsymbol{\gamma}_i$ as the particle absolute temperature and the chemical potential array of particle i, respectively. It should be noted that unlike equilibrium statistical mechanics, the temperature and chemical

potential fields need not be uniform anymore and may vary from particle to particle when the system is away from equilibrium.

2.2 Variational meanfield theory

Despite the formal simplicity of the non-equilibrium statistical model just mentioned above, it is generally intractable to calculate the thermodynamic potentials in a closed form, which leads to the need for approximation theory. Venturini et al. [8] have extended the classical variational meanfield theory to systems described by the proposed non-equilibrium statistical framework. The resulting variational framework provides a convenient basis for the formulation of computationally tractable models. Specifically, the maximum-entropy principle in Eq. (2) with local constraints is equivalent to the minimality of the functional of free entropy

$$F\left(\{h_0\},\{\beta\},\{\gamma\}\right)=k_{\mathrm{B}}\{\beta\}^{\mathrm{T}}\left\{\left\langle h-h_0\right\rangle_0\right\}-\Phi_0 \tag{6}$$

over some class H_0 of the local trial Hamiltonians $\{h_0\}$ with $\Phi_0 = k_{\mathrm{B}}\log\Xi_0$.

We are considering a binary system consisting of metal atoms occupying a perfect lattice whose interstitial sites are either empty or occupied by H atoms. For ease of reference, we designate the metal atoms in the system by means of an index set I_{M} and the H atoms by an index set I_{H}. For the system under consideration, the occupancy field $\{\boldsymbol{n}\}$ can be restricted to the interstitial sites, I_{H} since the metal sites are always occupied. Hence, M = 1, $\{n\} = \{n_i, i \in I_{\mathrm{H}}\}$ and $n_i = 0$ if the i-th interstitial site is empty and $n_i = 1$ if it is occupied by H atom. We restrict our attention to quasistatic process, so the Hamiltonian is fully determined by the interatomic potential. In order to obtain explicit formulations of thermodynamic potentials suitable for computations, we combine the effects of positions and fractions and apply the meanfield approximation theory with carefully designed trial Hamiltonians

$$V_0\left(\{\boldsymbol{q}\},\{n\}\right)=\sum_{i\in I_{\mathrm{M}}\cup I_{\mathrm{H}}}k_{\mathrm{B}}T_i\alpha_{0i}\left|\boldsymbol{q}_i-\bar{\boldsymbol{q}}_i\right|^2-\sum_{i\in I_{\mathrm{H}}}k_{\mathrm{B}}T_i\gamma_{0i}n_i \tag{7}$$

where $\{\bar{\boldsymbol{q}}\}$ are the meanfield values for atomic instantaneous positions. $\{\alpha_0\}$ and $\{\gamma_0\}$ are coefficients which need to be determined. We consider throughout isothermal conditions at fixed temperature T, so that $\beta_i = 1/(k_{\mathrm{B}}T_i)$ is uniform at all sites of the system. By calculating the meanfield value for H occupancy function $\{n\}$**,** we have

$$\gamma_{0i}=\log\frac{x_i}{1-x_i}-\gamma_i \tag{8}$$

where we have used the relation $x_i = \langle n_i\rangle_0, \forall i \in I_{\mathrm{H}}$, as the meanfield H atomic fraction.

By using Eq. (8), the free entropy function which needs to be minimized can be expressed as

$$\begin{aligned}F\left(\{h_0\},\{\gamma\}\right)=&\frac{1}{T}\left\langle V\right\rangle_0+\sum_{i\in I_{\mathrm{H}}}\left(k_{\mathrm{B}}\log\frac{x_i}{1-x_i}-k_{\mathrm{B}}\gamma_i\right)x_i+k_{\mathrm{B}}\sum_{i\in I_{\mathrm{H}}}\log\left(1-x_i\right)\\&+\frac{3}{2}k_{\mathrm{B}}\sum_{i\in I_{\mathrm{M}}\cup I_{\mathrm{H}}}\log\alpha_{0i}-\frac{3}{2}k_{\mathrm{B}}\sum_{i\in I_{\mathrm{M}}\cup I_{\mathrm{H}}}\left(1+\log\pi\right)\end{aligned} \tag{9}$$

where $V\{\{\boldsymbol{q}\},\{n\}\}$ is the interatomic potential.

2.3 Local equilibrium relations

The optimal values of $\{\bar{\boldsymbol{q}}\}$, $\{x\}$, and $\{\alpha_0\}$ can be obtained from the minimum grand-canonical free-entropy principle of Eq. (9). Adopting Euler-Lagrange equations, the optimality condition for meanfield atomic fraction $\{x\}$ can give the relation for nondimensional chemical potential

$$\gamma_i = \log\frac{x_i}{1-x_i} + \frac{1}{k_B T}\frac{\partial\langle V\rangle_0}{\partial x_i} \tag{10}$$

This form of chemical potential characterizes the instantaneous state of a system and provides driving forces for its evolution. When calculating the chemical potential of one H site, unlike the classical entropy-of-mixing relation that is only based on the fraction of its own atomic site, this novel model not only considers the effective neighboring H sites, but also includes the deformation of the lattice structure.

2.4 Discrete kinetic laws

This thermodynamics model just described is then coupled with discrete kinetic laws of Onsager type which governs mass transport. Actually, this defines the evolution of H fraction, whose characteristic computational time step is much greater than femtosecond. In this work, we consider linear models of the form

$$\dot{x}_i = -\sum_{j\in I_{\mathrm{H}},\, j\neq i} B_{ij} x_{ij} k_{\mathrm{B}} \left(\gamma_i - \gamma_j\right), \quad i \in I_{\mathrm{H}} \tag{11}$$

where $x_{ij} = \left(x_i + x_j\right)/2$ and B_{ij} is the bondwise diffusivity coefficient between the i and j atomic pair.

To sum up, the computational framework of the deformation-diffusion coupled analysis of H diffusion in nanomaterials is shown in Fig. 1, where t_n denotes the n-th time step.

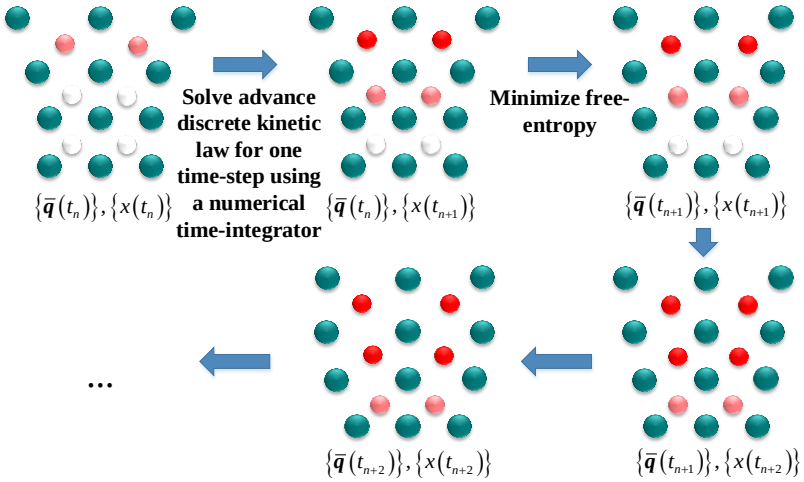

Figure 1: The computational framework of the deformation-diffusion coupled analysis.

3 APPLICATION TO PALLADIUM NANOFILMS

Since the feasibility of the described method depends critically on the formulation of computationally tractable average of the interatomic potential, we proceed to assess the fidelity of such models by direct comparison with experimental observation. To this end, we specifically investigate the palladium-hydrogen (Pd-H) system. It has been known that the Pd-H system

exists in two different phases: the α-phase at a low H concentration (up to $PdH_{0.015}$), and the β-phase at a high H concentration ($PdH_{0.607}$ and above). In the process of the α/β-phase transition, there is a lattice expansion leading to about 10.4% increase in volume [12]. It is noted that the Pd sub-lattice remains face-centered cubic (FCC) in both α and β phases, while the H atoms occupy interstitial octahedral sites, which themselves also define a second FCC sub-lattice.

3.1 Computational model

We focus on the EAM potential for Pd-H system proposed in Ref. [13]. In order to simplify calculations, we use the quadratic polynomial to approximate the EAM potential. By using Jensen's inequality, the meanfield average of the simplified EAM is of the form

$$\begin{aligned}\langle V\rangle_0 = A+\sum_{i\in I_{\mathrm{H}}} B_i x_i + \sum_{i,j\in I_{\mathrm{Pd}},i\neq j} C_{ij}\langle r_{ij}\rangle_0 + \sum_{i,j\in I_{\mathrm{H}},i\neq j} D_{ij}x_i x_j + \sum_{i\in I_{\mathrm{H}},j\in I_{\mathrm{Pd}}} E_{ij}x_i\langle r_{ij}\rangle_0 \\ + \sum_{i,j\in I_{\mathrm{Pd}},i\neq j} F_{ij}\langle r_{ij}\rangle_0^2 + \sum_{i,j\in I_{\mathrm{H}},i\neq j} G_{ij}x_i x_j\langle r_{ij}\rangle_0 + \sum_{i\in I_{\mathrm{H}},j\in I_{\mathrm{Pd}}} H_{ij}x_i\langle r_{ij}\rangle_0^2 + \sum_{i,j\in I_{\mathrm{H}},i\neq j} I_{ij}x_i x_j\langle r_{ij}\rangle_0^2\end{aligned} \tag{12}$$

Inserting the parameterization and calibration provided in Ref. [13], for T = 300 K, we have $A = -12.9356$ eV and $B_i = 3.2448$ eV. The other coefficients in Eq. (12) are listed in Table 1, where $N_i^{(k)}$ denotes the k-th shell of neighbors of site i.

	C_{ij} (eV/Å)	D_{ij} (eV)	E_{ij} (eV/Å)	F_{ij} (eV/Å^2)	G_{ij} (eV/Å)	H_{ij} (eV/Å^2)	I_{ij} (eV/Å^2)
$j \in N_i^{(1)}$	−1.1529	0.5956	−0.1496	0.2016	−0.3971	0.0574	0.0658
$j \in N_i^{(2)}$	0.2684	−0.0459	0.1940	−0.0225	0.0203	−0.0296	−0.0022
$j \in N_i^{(3)}$	0.3642	−0.0500	−0.1307	−0.0315	0.0207	0.0120	−0.0021

Table 1: Coefficients in the simplified EAM potential.

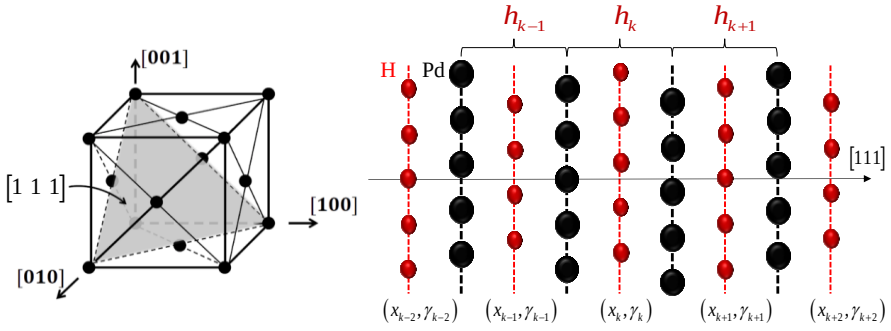

Figure 2: 1D diffusion and 3D deformation problem.

Specifically, we investigate the H diffusion problem in Pd nanofilms. Since the size of the surface area is much greater than the thickness, the H diffusion process is essentially one-dimensional in the thickness direction, that is, the [111] direction as shown in Fig. 2. But the lattice deformation is three-dimensional. As a result, the H atomic fractions $\{x\}$ and the non-dimensionalized chemical potential $\{\gamma\}$ can be constant on each [111] H plane of the FCC sub-lattice. Let N be the number of [111] planes in a specific film. We denote through x_k and γ_k, k = 1, 2, …, N, the H atomic fraction and nondimensional chemical potential on the k-th [111] plane. At the same time, it is assumed that the average instantaneous position of each atomic site can be fully determined by the average Pd plane distances $\{h\}$. That is, the average distance between any atoms is the function of average Pd plane distances along the diffusion direction. As the result, the local equilibrium relation about deformation is equal to minimizing meanfield

interatomic potential with respect to average Pd plane distances. The nominal lattice constant at the *k*-th plane is defined as $a_k = \sqrt{3}h_k$ for Pd [1 1 1] nanofilms in this work.

3.2 Model validation in equilibrium properties

The equilibrium relation of nondimensional chemical potential in Eq. (10) is plotted in Fig. 3 for a uniform H fraction, compared with the classical relation $\gamma = \log(x)$ derived from the entropy of mixing. Obviously, the proposed model exhibits an up-down-up equilibrium relation characteristic of phase transitions. In detail, the two local extreme points can be regarded as the α and β phases of the Pd-H system, respectively. The ability of the proposed model to predict the phase transition of Pd-H in the process of H diffusion will be further investigated.

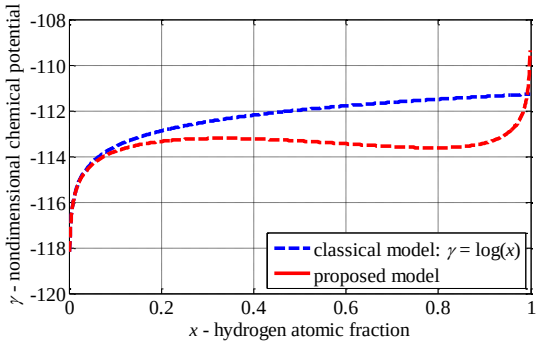

Figure 3: Comparison of equilibrium chemical potential between the proposed model and the classical relation $\gamma = \log(x)$.

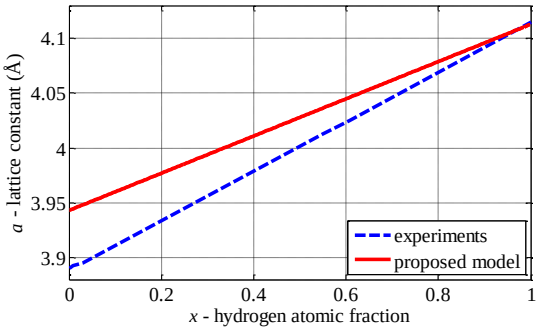

Figure 4: Comparison of equilibrium lattice constant between the proposed model and the experiments.

The equilibrium relation of lattice constant in the proposed model is compared with the experimental one from Ref. [14] in Fig. 4. The experimental points are connected by dashed lines in order to guide eye. It can be found that the trend of an increasing equilibrium lattice constant with the increasing of H fraction is predicted clearly by our proposed model. The difference between simulation and experiment results is a little greater during the low concentration and decreases gradually with the increase of H fraction, nevertheless.

3.3 Specific discrete kinetic equation

In order to describe the time-dependent H diffusion in Pd nanofilms, the general discrete kinetic law should be specified in one-dimensional direction. Restricting mass transport to the nearest shell of neighbors and using Taylor expansion, we express x_j and γ_j about x_i and γ_i. Then considering FCC Pd lattice crystal and [1 1 1] H diffusion direction, the discrete kinetic equation is of the form

$$\dot{x}_k = \frac{3}{2} k_{\mathrm{B}} \left[\left(x_k + x_{k-1} \right) \left(\gamma_{k-1} - \gamma_k \right) B_{k,k-1} + \left(x_k + x_{k+1} \right) \left(\gamma_{k+1} - \gamma_k \right) B_{k,k+1} \right] \tag{13}$$

for k = 2, 3, …, N−1. $B_{k,k-1}$ denotes the bondwise diffusivity coefficient between k-th and (k−1)-th H planes, which can be computed through solving the matrix equation by comparison with Fick's second law

$$\begin{bmatrix} 3\left(h_{k-2}+2h_{k-1}+h_k\right)^2 & 18\left(h_{k-1}+2h_k+h_{k+1}\right)^2 & 3\left(h_k+2h_{k+1}+h_{k+2}\right)^2 \\ 3\left(h_{k-1}+h_k\right)^2 & 0 & 3\left(h_k+h_{k+1}\right)^2 \\ -\left(h_{k-1}+h_k\right) & 0 & h_k+h_{k+1} \end{bmatrix} \begin{bmatrix} B_{k,k-1} \\ B_{k,k} \\ B_{k,k+1} \end{bmatrix} = \frac{8D_{\mathrm{H}}}{k_{\mathrm{B}}} \begin{bmatrix} 16 \\ 1 \\ 0 \end{bmatrix} \tag{14}$$

where D_{H} is the isotropic macroscopic diffusivity constant for H in Pd. The equilibrium relation of Eq. (14) is plotted in Fig. 5. It can be found that the decreasing trend of bondwise diffusivity coefficient with increasing plane distance is predicted. This trend is intense during mall plane distances and then becomes moderate gradually.

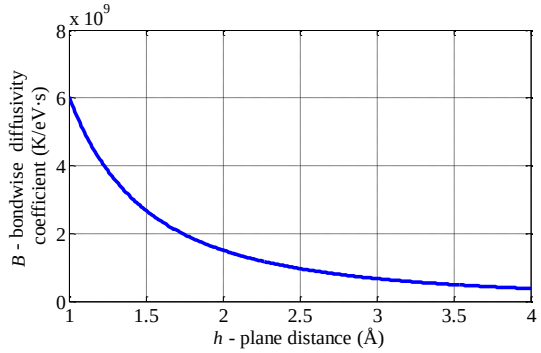

Figure 5: Equilibrium relation of bondwise diffusivity coefficient.

3.4 Model validation for hydrogen desorption

We simulate the nanofilms of thickness $L = 460$ Å and 1350 Å. Eq. (13) is calculated by the following initial and boundary conditions based on the experimental set-up

$$\begin{cases} x_k(0) = x_0, & k = 2,3,\ldots,N \\ x_1(t) = x^*, & 0 \le t \le t_{\max} \\ x_{N-1}(t) = x_N(t), & 0 \le t \le t_{\max} \end{cases} \tag{15}$$

where x_0 denotes the initial uniform H atomic fraction in the film interior, and x^* denotes the fixed H atomic fraction at the film surface in contact with the electrolyte solution. No-flux boundary condition is imposed at the other side of the nanofilms, since H diffusion between the Pd film and the gold-coated nickel substrate is negligible. x^* can be determined according to Ref. [9], and x_0 is set to 0.009 in the computation based on the measurement [15] in both cases. All the case-dependent coefficients used in the simulations are reported in Table 2.

	L (Å)	N (Å)	x^*	D_{H}(Å²/s)
Case I	460	204	0.0019	2.1×10^5
Case II	1350	595	0.0047	1.56×10^6

Table 2: Case-dependent coefficients used in H desorption simulations.

Eq. (13) is discretized in time by the mid-point rule which has second-order accuracy. The computational time steps are set to $\Delta t = 5.0 \times 10^{-6}$ s and 1.0×10^{-6} s in Case I and II, respectively. The maximum simulation time for both cases is $t_{\max} = 1.0$ s.

The spatial variation of H atomic fraction on the surface of nanofilms is converted into electric current using the relation in Ref. [16]. The results are plotted in Fig. 6 in comparison with the experimental data reported in Ref. [17] at T = 300 K. It is obvious that in both cases, the predicted electric current agrees well with the experimental measurements with regard to both the initial transient and the long-term behavior.

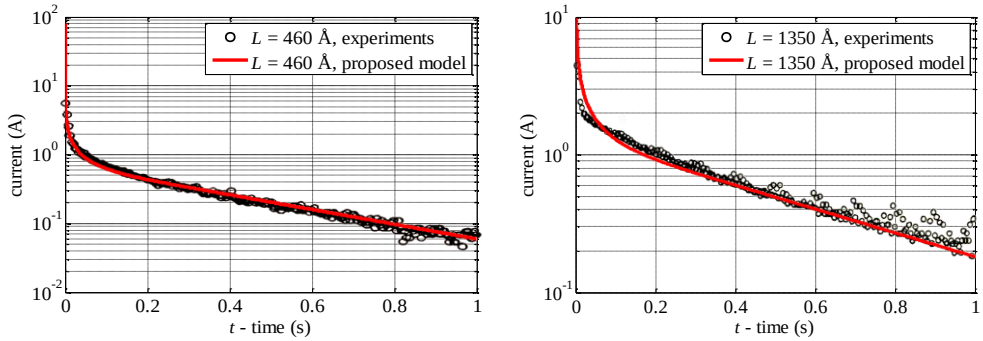

Figure 6: Comparison of experimental and predicted results for current on the surface. (a) 460 Å Pd nanofilms. (b) 1350 Å Pd nanofilms.

3.5 Prediction for phase transition

As discussed in Fig. 3, the equilibrium condition of Eq. (10) is able to capture the phase characteristic of one Pd-H system. Here, we further investigate this ability by taking the Pd-H system into its β-phase, and highlight the capability of the proposed computational model as to capturing complicated phase transition in a very slow diffusion process which has time scale of seconds. We simulate H absorption in the Pd nanofilms with the thickness $L = 460$ Å characterized by a high H fraction on the surface $x^* = 0.99$. Using the deformation-diffusion coupled model proposed in this paper, the H atomic fractions and lattice constants at six time points are plotted in Fig. 7, respectively. Also, the similar figures through the classical mixing-entropy relation $\gamma = \log(x)$ are shown in Fig. 8 for comparison. Clearly, the H diffusion process in Pd lattice structure is characterized by the propagation of an α/β-phase boundary: the α-phase about $PdH_{0.165}$ and $a = 3.968$ Å, and the β-phase about $PdH_{0.898}$ and $a = 4.098$ Å. This phase propagation cannot be observed by using the classical relation $\gamma = \log(x)$. Moreover, the lattice expansion in the α/β-phase transition is about 3.27%, which gives rise to about 9.83% increase in volume. This value is close to that observed in previous experiments. Nevertheless, the H atomic fractions at α/β-phase are greater than those obtained from experiments, which is probably due to the EAM potential we adopt.

Fig. 9 shows the deformation-diffusion coupled process of H absorption at several time steps in the part of the deformed Pd lattice structure, where the big spheres denote Pd sites and the small ones are H sites. It can be seen that the lattice structure will expand in three dimensions as H atoms diffuse in [1 1 1] direction. Obviously there exists a phase boundary between the domains with high and low H atomic fractions. As a result, the capability of the proposed model in predicting the phase transition in a long-term process is remarkable.

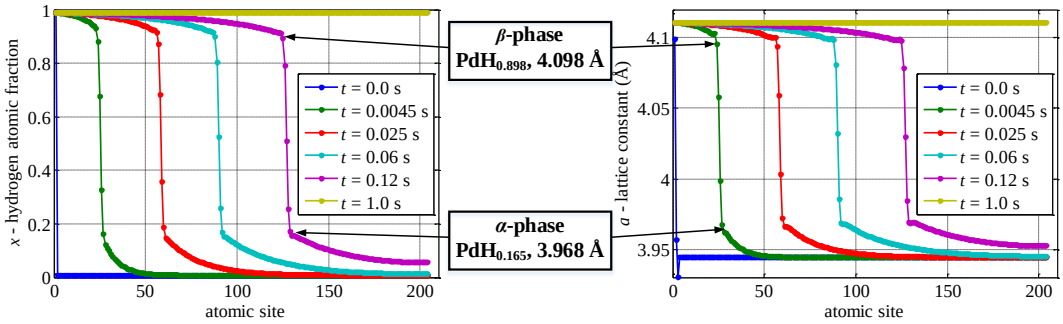

Figure 7: H absorption in 460 Å Pd nanofilms by the proposed model. (a) H atomic fraction. (b) Lattice constant.

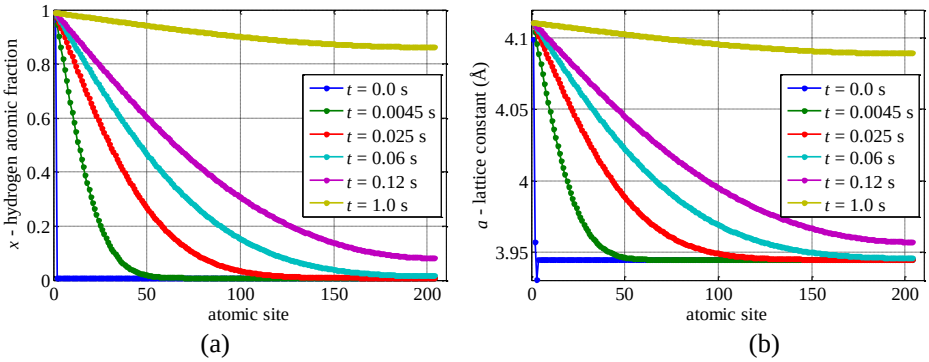

Figure 8: H absorption in 460 Å Pd nanofilms by the classical relation $\gamma = \log(x)$. (a) H atomic fraction. (b) Lattice constant.

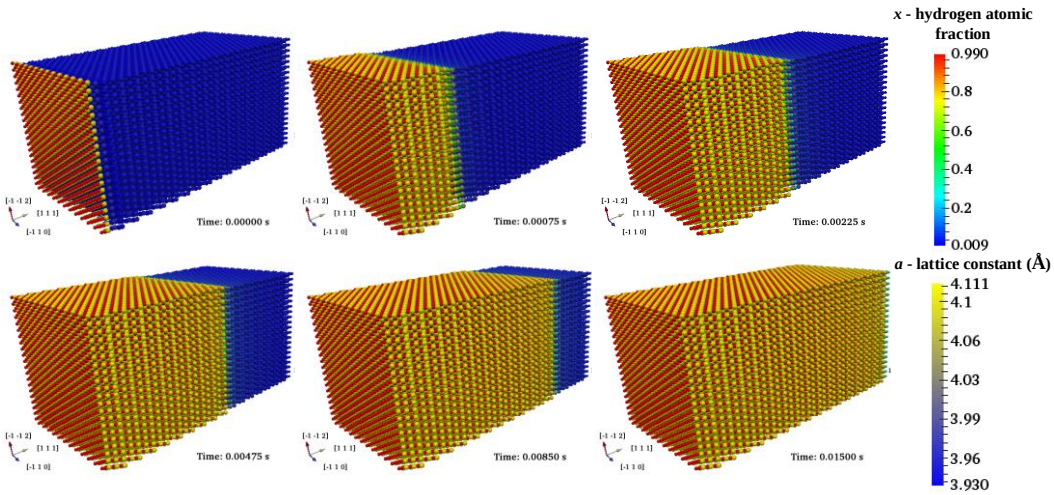

Figure 9: Deformation-diffusion coupled process of H absorption in Pd nanofilms.

4 SUMMARY AND CONCLUDING REMARKS

We have applied the theory of non-equilibrium statistical thermodynamics to the study of hydrogen absorption and desorption in metal-based nanomaterials, while maintaining a strictly atomistic description of the metal material. We have proposed a new form of trial Hamiltonians and combined it with the specific discrete kinetic law for hydrogen diffusion in palladium nano-films. The coupled thermodynamic and kinetic models are solved numerically in a partitioned

procedure using explicit time-integrators. The proposed model has been validated in both equilibrium and non-equilibrium cases, and the computational results are compared with those by classical chemical potential relation derived from entropy-of-mixing. Our model can have a good agreement with the experimental measurements in hydrogen desorption process and predict the phase boundary transition of hydrogen absorption with the well-known volume expansion. The results demonstrate that the presented computational framework is capable of capturing phase-change and phase-dependent diffusion of hydrogen in a deformed metal structure as part of a long-term analysis.

REFERENCES

[1] W. Li, C. Li, H. Ma, J. Chen, Magnesium nanowires: enhanced kinetics for hydrogen absorption and desorption. *Journal of the American Chemical Society*, **129**, 6710-6711, 2007.

[2] D. Delafosse, T. Magnin, Hydrogen induced plasticity in stress corrosion cracking of engineering systems. *Engineering Fracture Mechanics*, **68**, 693-729, 2001.

[3] K.A. Williams, P.C. Eklund, Monte Carlo simulations of H-2 physisorption in finite-diameter carbon nanotube ropes. *Chemical Physics Letters*, **320**, 352-358, 2000.

[4] V.J. Surya, K. Iyakutti, H. Mizuseki, Y. Kawazoe, First principles study on desorption of chemisorbed hydrogen atoms from single-walled carbon nanotubes under external electric field. *International Journal of Hydrogen Energy*, **36**, 13645-13656, 2011.

[5] R.A. Miron, K.A. Fichthorn, Accelerated molecular dynamics with the bond-boost method. *The Journal of Chemical Physics*, **119**, 6210-6216, 2003.

[6] I. Brihuega, O. Custance, J.M. Gómez-Rodríguez, Surface diffusion of single vacancies on Ge (111) - c (2×8) studied by variable temperature scanning tunneling microscopy. *Physical Review B*, **70**, 165410, 2004.

[7] J. Li, S. Sarkar, W.T. Cox, T.J. Lenosky, E. Bitzek, Y. Wang, Diffusive molecular dynamics and its application to nanoindentation and sintering. *Physical Review B*, **84**, 054103, 2011.

[8] G. Venturini, K.G. Wang, I. Romero, M.P. Ariza, M. Ortiz, Long-term simulation of heat and mass transport in alloys at finite temperature. *Journal of the Mechanics and Physics of Solids*, **73**, 242-268, 2014.

[9] K.G. Wang, M. Ortiz, M.P. Ariza, Long-term atomistic simulation of hydrogen diffusion in metals. *International Journal of Hydrogen Energy*, **40**, 5353-5358, 2015.

[10] E.T. Jaynes, Information theory and statistical mechanics I. *Physical Review*, **106**, 620-630, 1957.

[11] E.T. Jaynes, Information theory and statistical mechanics II. *Physical Review*, **108**, 171-190, 1957.

[12] R.J. Wolf, M.W. Lee, R.C. Davis, P.J. Fay, J.R. Ray, Pressure-composition isotherms for palladium hydride. *Physical Review B*, **48**, 12415, 1993.

[13] X.W. Zhou, J.A. Zimmerman, B.M. Wong, J.J. Hoyt, An embedded-atom method interatomic potential for Pd-H alloys. *Journal of Materials Research*, **23**, 704-718, 2008.

[14] Y. Sakamoto, K. Yuwasa, K. Hirayama, X-ray investigation of the absorption of hydrogen by several palladium and nickel solid solution alloys. *Journal of the Less Common Metals*, **88**, 115-124, 1982.

[15] H. Hagi, Diffusion coefficient of hydrogen in palladium films prepared by RF sputtering. *Materials Transactions, JIM*, **31**, 954-958, 1990.

[16] N. Boes, H. Züchner, Electrochemical methods for studying diffusion, permeation and solubility of hydrogen in metals. *Journal of the Less Common Metals*, **49**, 223-240, 1976.

[17] Y. Li, Y.T. Cheng, Hydrogen diffusion and solubility in palladium thin films. *International Journal of Hydrogen Energy*, **21**, 281-291, 1996.